Journal of Asian Earth Sciences 117 (2016) 52–63

Contents lists available at ScienceDirect

Journal of Asian Earth Sciences

journal homepage: www.elsevier.com/locate/jseaes

# Crustal and upper-mantle structure of the southeastern Tibetan Plateau from joint analysis of surface wave dispersion and receiver functions

Mengkui Li [a], Shuangxi Zhang [a,b,c,*], Fang Wang [a], Tengfei Wu [a], Weibing Qin [a]

[a] Department of Geophysics, School of Geodesy and Geomatics, Wuhan University, Wuhan 430079, China
[b] Key Laboratory of Geospace Environment and Geodesy of Ministry of Education, Wuhan University, Wuhan 430079, China
[c] Collaborative Innovation Center of Geospace Information Science, Wuhan University, Wuhan 430079, China

ARTICLE INFO

*Article history:*
Received 24 August 2015
Received in revised form 24 November 2015
Accepted 2 December 2015
Available online 8 December 2015

*Keywords:*
Southeastern Tibetan Plateau
Joint analysis
Receiver function
Surface wave dispersion
Crustal flow

ABSTRACT

Researches on the southeastern Tibetan Plateau provide important insights into the tectonic evolution of the Tibetan Plateau. In this study, we have constructed a high-resolution 3D shear-wave velocity model through joint inversion of receiver functions and surface wave dispersion data. The crustal thickness and Poisson's ratio models are first determined by *H*–*k* stacking of receiver functions. The crustal thickness changes from 30 km in the south to 62 km in the north, presenting strong lateral variations. The fundamental mode of Rayleigh wave dispersion data spanning periods from 8 to 65 s were then jointly used to constraint the absolute shear-wave velocity. The shear-wave velocity structure shows lateral variations. There are low velocity zones distributed in the crust and upper mantle. Two continuously distributed low velocity zones are clearly presented in the middle-to-lower crust, which extend from north toward southeast and southwest, respectively, joining together in southern Yunnan. In this study, we deduced the migration model of soft materials in middle-to-lower crust in southeastern Tibetan Plateau, which explains that the resistance from Sichuan Basin separates the flowing materials from Tibetan Plateau into southeast and northwest branches. They flow along the west margin of Sichuan Basin and then extrude out from northeastern and southeastern Tibetan Plateau respectively. The southeast branch is blocked and cannot flow in the entire crust. It is limited in a certain range of depths and channels. The two low velocity zones in this study possibly present two flow channels of the middle-to-lower crustal materials extruded from the Tibetan Plateau.



## 1. Introduction

The continent-to-continent collision between the Indian and Eurasian Plates began about 50 Ma ago causing the uplift, crustal shortening and thickening of the Tibetan Plateau (TP; Yin and Harrison, 2000; Royden et al., 2008; Hubbard and Shaw, 2009). TP evolution has been a fascinating topic for geoscientists (Tapponnier et al., 1982; Lev et al., 2006; Xu et al., 2007; Cook and Royden, 2008; Royden et al., 2008; Huang et al., 2010, 2015; Yao et al., 2008, 2010; Zhao et al., 2011; Chen et al., 2013; Bao et al., 2015). During the early stages of collision, the tectonic evolution was dominated by the crustal thickening, while in the past 10–15 Ma, the lateral extrusion has become dominant (Royden et al., 2008; Chen et al., 2013). Resistance from the Sichuan Basin (SB) to the eastward expansion of the TP makes the lateral extrusion of the crustal materials to the southeastern and northeastern TP (Yao et al., 2010). Therefore, the southeastern Tibetan Plateau (SETP) becomes an important passageway for materials moving toward southeast. Unfortunately, current studies have not yet discovered the details of the passageway.

This study focuses on the area from the southeastern part of the TP to southern Yunnan, as shown in Fig. 1. The research region is located between the eastern Himalayan syntaxis (EHS) and the mechanically rigid SB. Its deformation is jointly influenced by the northward subduction of the Indian plate and the eastward subduction of the Burmese microplate (Yin and Harrison, 2000; Li C. et al., 2008). The area is the southern end of the South North seismic belt of China, so it has a complex tectonic background and high level of seismicity (Wu et al., 2001; Hu et al., 2003; Li Y.H. et al., 2008). It is of significant academic interest for the studies of shear-wave velocity ($V_S$) structure. GPS velocity measurements show a clockwise crustal material motion around EHS (Wang et al., 2001; Zhang et al., 2004; Gan et al., 2007), which implies the existence of material extrusion in SETP. Several models have

* Corresponding author at: Department of Geophysics, School of Geodesy and Geomatics, Wuhan University, Wuhan 430079, China.
*E-mail address:* shxzhang@sgg.whu.edu.cn (S. Zhang).

http://dx.doi.org/10.1016/j.jseaes.2015.12.002
1367-9120/

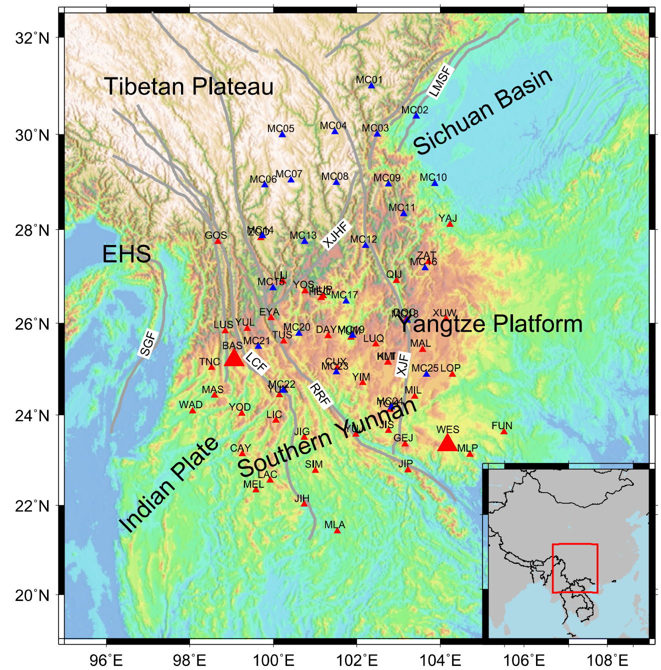


**Fig. 1.** Tectonic map of SETP. The red triangles are 46 seismic stations operated by the Earthquake Administration of Yunnan Province. The blue triangles are 25 seismic stations deployed by MIT and Chengdu Institute Geology and Mineral Resources. The larger red triangles mark the locations of two example stations used in the text. Gray lines are some representative faults in this area. EHS: Eastern Himalayan Syntaxis; SGF: Sagaing fault; LCF: Langcangjiang fault; RRF: Red-river fault; XJF: Xiaojiang fault; XJHF: Xiaojinhe fault; LMSF: Longmenshan fault. Inset map: location of the color imaged study region. ETOPO1 model is used to generate the color imaged topography. (For interpretation of the references to color in this figure legend, the reader is referred to the web version of this article.)

been proposed to explain the deformations of the eastern and southeastern TP, such as lateral extrusion of rigid blocks (Tapponnier et al., 1982, 2001), continuous deformation of the entire lithosphere (England and Houseman, 1986; Yang and Liu, 2013), and the ductile channel flow in the middle/lower crust (Clark and Royden, 2000; Royden et al., 1997, 2008). Among these models, the channel flow model is the most accepted one in seismology community (Wang et al., 2010; Yao et al., 2010; Sun et al., 2012; Bao et al., 2015). However, the deformation mechanism and the spatial extension of the flow channels, are still unclear and controversial (Clark and Royden, 2000; Cook and Royden, 2008; Bai et al., 2010; Sun et al., 2012; Bao et al., 2015). Such mechanisms are also related to the local earthquakes and the tectonic evolution of TP (Xu et al., 2007; Yao et al., 2010; Bao et al., 2015).

Understanding the details of the crustal and upper-mantle $V_S$ structure, such as the distribution of low velocity zones (LVZs), can provide essential information about the competing models, such as the most accepted flow channel model (Yao et al., 2010; Bao et al., 2015; Huang et al., 2015). It would be greatly helpful to reveal the possible existence of the flow channels and their spatial distribution. Materials in LVZs are relatively soft and prone to move under lateral extrusion. Continuously distributed LVZs implies the potential channels for material flow. In the present study, we firstly provide a crustal thickness and Poisson's ratio model from teleseismic *P*-wave receiver functions (RFs) by *H*–*k* stacking approach (Zhu and Kanamori, 2000). According to the Poisson's ratio model, a 3D $V_S$ structure is constructed from 1D joint inversion of RFs and surface wave dispersion data (SWD) at each station (Julià et al., 2000; Herrmann and Ammon, 2002; Sosa et al., 2014). Finally, a tectonic model is proposed for material flow in SETP and some possible tectonic implications are discussed.

## 2. Data

The continuous waveform data recorded by 71 regionally distributed broadband stations were used to calculate the radial RFs. These stations consist of two parts; 46 stations belong to the Yunnan networks with recordings from 2011 to 2013 (red triangles in Fig. 1) and 25 stations located between EHS and SB (blue triangles in Fig. 1) which were deployed by MIT and Chengdu Institute of Geology and Mineral Resources with recordings from 2003 to 2004 (Yao et al., 2008; Huang et al., 2010). We selected events having moment magnitudes between 5.5 and 7.5 within epicentral distances from 30° to 90°. The selection criteria ensured good signal to noise ratios (SNR), minimum influence of source complexity and waves are steeply incident. Fig. 2 shows the events distribution of BAS station as an example (after preliminary selection during RFs calculation). The station has good azimuthal coverage events, although most of the events are from Pacific Ocean direction. The SWD data were taken from the surface wave study carried by Xie et al. (2013), in which the precise Rayleigh wave phase velocity spanning periods from 8 to 65 s were determined from ambient noise tomography. The pure path dispersion data at each station was interpolated from the surface wave tomography model, and used as the SWD dataset for joint inversion.

## 3. Methodology

### 3.1. Calculation of P-wave RFs

The radial *P*-wave RFs were calculated by deconvolving the vertical components from the horizontal components of teleseismic waveforms. This approach is able to isolate the receiver site effect from source signature and other effects (Ammon, 1991; Ammon and Zandt, 1993). By following the processing steps of Wang et al. (2010), we firstly removed the trend and the mean value from the waveforms. After that, we band-pass filtered the waveforms using a Butterworth Filter with corner values of 0.05 and 2.0 Hz. The waveforms were then resampled to 10 sps, rotated from north and east components to radial and transverse components. Without consideration of the possible anisotropy and Moho dipping, the transverse components waveforms were discarded (Xu et al., 2007; Macpherson et al., 2012, 2013). Thirdly, we manually picked the *P*-wave arrivals and cut time window with 20 s before and 120 s after *P*-wave arrivals. In order to collect as many data as possible, we did not perform strict data quality control on raw waveforms. Further quality controls of RFs were performed during *H*–*k* stacking and 1D structure inversions. Finally, the vertical component was deconvolved from the radial component by using a time-domain iterative deconvolution technique (Ligorria and Ammon, 1999), which is based on least square minimization of the difference between the observed and predicted horizontal component waveforms. Gaussian width factors of 1.5 and 2.0 were selected to attenuate the frequencies greater than about 0.75 and 1.0 Hz. The RFs with waveform fits less than 85% were discarded. This procedure is hereinafter referred as preliminary selection. Fig. 3 shows the RFs of BAS and WES stations with Gaussian width factor 1.5 as examples after the preliminary selection (black and blue curves). The coherent RFs were further selected by using the cross-correlation matrix method (Tkalčić et al., 2006, 2011) described below.

### 3.2. Cross-correlation matrix method for RF selection

The subjectively selected RFs, which may cause the distortion and lacking of some representative features, cannot be stacked for an averaged RF directly (Chen et al., 2010; Tkalčić et al., 2011). We took a statistical approach to select only mutually